UKACC International Conference on Control 2012
Cardiff, UK, 3-5 September 2012

Modeling and Simulation of a Coupled Double-Loop-Cooling System for PEM-Fuel Cell Stack Cooling

Martin Schultze, Michael Kirsten, Sven Helmker and Joachim Horn
Institute for Control Engineering
Helmut-Schmidt-University Hamburg
D-22043 Hamburg, Germany

Abstract—**PEM (Polymer electrolyte membrane) fuel cell systems are very efficient energy converters. They generate electrical power, low oxygen concentration cathode exhaust gas, water as well as heat. The fuel cell technology has become very attractive for the use on aircraft where it may serve as a replacement for the auxiliary power unit currently being used for generating electrical power. For the use on aircraft coupled double-loop-cooling systems are investigated as different coolants can be used for inner and outer cooling system. As fuel cell electrical power is nonlinearly dependent on stack temperature and current, a cooling temperature control is required.**

In this study a nonlinear simulation model of a coupled double-loop-cooling system is presented. The effectiveness-NTU method is used to model the intercooler that couples inner and outer cooling loop. This method has the advantage that outlet temperatures are obtained explicitly based on inlet coolant temperatures and cooling mass flows. The model is valid over the entire operating range of the hydrogen fed fuel cell system. Subsequently, a linear controller with feedforward control is proposed to control for the stack inlet cooling temperature.

PEM fuel cell system model; nonlinear heat exchanger model; model identification; fuel cell temperature control

I. INTRODUCTION

For aircraft applications the fuel cell technology is investigated regarding to its multifunctional use. One of its main aspects is the use of oxygen depleted cathode exhaust air (ODA) for tank inerting [1]. For this purpose the oxygen content needs to be close or less than 10% (vol.) [2]. Another and certainly one of the most important aspects of the multifunctional use is electrical power generation. So far, auxiliary power units (APU) generate electrical power for the use on aircraft during ground operations. An APU, though, is a significant source of green house gases such as CO_2 and NO_x and noise. Therefore, hydrogen-gas fed PEM fuel cell systems are studied as a replacement for APUs to significantly reduce these pollutants. Among the different types of fuel cells, PEM fuel cells are the most suitable ones for dynamic applications. Nonetheless, proper fuel cell system operation such as a well humidified membrane or a proper supply of reactant gases and well kept gas pressure is central for a maximum fuel cell lifetime [3]. In this study a fuel cell system with anode hydrogen recirculation for stack humidification is used. Proper fuel and air supply as well as the temperature difference across the stack is managed by an internal fuel cell system controller. The fuel cell system is connected to a controllable ohmic load that draws a current as requested. A schematic of the fuel cell system and its coupled two-loop-cooling system is shown in figure 1.

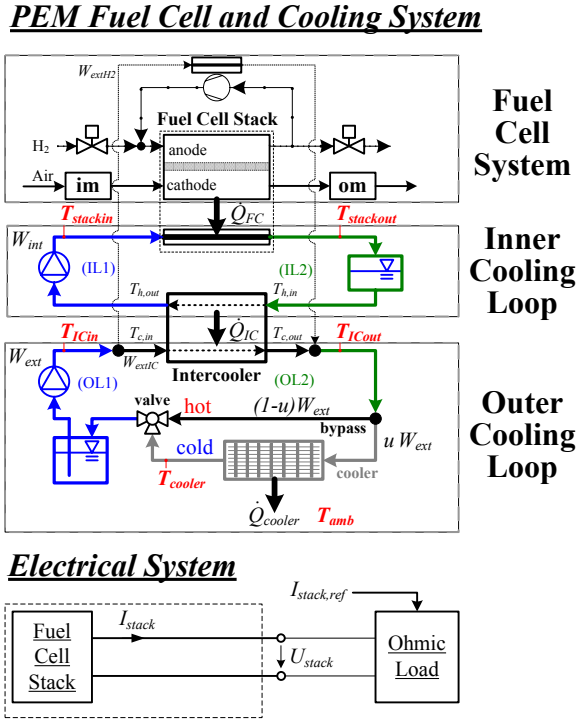

Figure 1. Schematic of the fuel cell system and the connected double-loop cooling system; the fuel cell system comprises the fuel cell stack, inlet and outlet manifolds and anode hydrogen recirculation; the cooling system comprises the inner and outer loop that are interconnected by a counter-flow heat exchanger, connecting pipes, a cooling valve and a cooler; heat flows from stack into the inner loop, inside the intercooler and in the cooler are shown (top); the fuel cell system is connected to an ohmic load (bottom)

The fuel cell system simulation model is based on models reported of in [4], [5] and [6]. Furthermore, product water leaves the fuel cell cathode as vapor and liquid. This has an influence on stack temperature and is taken into account as presented in [7] and [8]. The fuel cell system model is briefly outlined in section Simulation Model. The cooling system is modeled based on first principles. Heat exchanger models as

This study as part of the project "cabin technology and multifunctional fuel cell systems" has been supported by Airbus and the German Federal Ministry of Education and Research (support code: 03CL03A).

proposed in [9] and [6] are restricted on operating range. The effectiveness-NTU method [10] provides nonlinear models for several designs of heat exchangers. Ref. [11] uses this approach for a single-loop cooling system of an automotive fuel cell system assuming constant heat exchanger effectiveness. Constant effectiveness, however, might not hold true for the entire operating range. Here, the effectiveness-NTU method with mass flow dependent effectiveness is used to develop an intercooler model for the coupled double-loop-cooling system. The fuel cell system and intercooler model have been fit to experimental data, which is presented in section Model Identification. Actuating the cooling valve in the outer loop influences the stack inlet temperature in the inner cooling loop. To operate the fuel cell system at a certain stack inlet temperature a temperature controller with feedforward control is proposed in section Controller Design. A simulation of the nonlinear fuel cell and cooling system model with temperature controller are presented in section Simulation results.

II. SIMULATION MODEL

The overall system simulation model consists of a model of the fuel cell system, a model of its internal fuel cell system controller and a model of the controllable ohmic electrical load to which the fuel cell system is connected. A list of the model parameters is given in table 1 at the end of this paper. Inlet air is taken from an air pressure tank that is filled by a compressor. After compression air is cooled, dried and oil-filtered.

A. Fuel Cell System Model

The fuel cell system model comprises the fuel cell stack, a mass flow controller (MFC) for cathode air supply and the anode hydrogen recirculation for better hydrogen utilization and stack humidification. The internal fuel cell system controller operates the mass flow controller such that it delivers an air mass flow as specified by stoichiometry and stack current drawn. Furthermore, the internal controller operates the cooling pump in the inner cooling loop to set the reference temperature difference across the fuel cell stack. Inlet air is modeled as a dry and ideal gas consisting of 21% (vol.) oxygen and 79% (vol.) nitrogen. It has constant temperature.

1) Inlet Manifold Model

Inlet manifold pressure p_{im} (1) is gained by a pressure differential equation (γ=*1.4* [5]). In- and outlet temperature are assumed to be equal and constant. Flow W_{im} of dry air exiting the manifold is modeled by a linear nozzle equation (2) with nozzle constant k_{im} and the pressure difference of manifold and cathode pressure p_{ca}. Mass flow of dry air W_{MFC} (3) entering the manifold is supplied by a mass flow controller, which is modeled as a first order transfer function with time constant T_{MFC}. The mass flow reference is calculated using the reference stoichiometry λ_{ref} and the stack current I_{stack} being drawn.

$$\frac{dp_{im}}{dt} = \frac{\gamma R_{air}}{V_{im}} T_{im}\left(W_{MFC} - W_{im}\right) \tag{1}$$

$$W_{im} = k_{im}\left(p_{im} - p_{ca}\right) \tag{2}$$

$$W_{MFC} = \frac{1}{T_{MFC}s + 1}\left[I_{stack}\lambda_{ref}\left(M_{O2} + \frac{0.79}{0.21} M_{N2}\right)\frac{n_{cells}}{4F}\right] \tag{3}$$

2) Outlet Manifold Model

Vapor mass flow is obtained by water loading (4) of the dry gas mass flow. Water loading depends on total gas pressure p_i and vapor partial pressure $p_{i,v}$ (5), which solely depends on temperature [12]. Mass flows of water vapor $W_{ca,v}$, oxygen depleted air $W_{ca,oda}$ and liquid water $W_{ca,l}$ are supplied to the outlet manifold at stack temperature T_{stack}. The manifold is considered perfectly insulated. Mass flows $W_{om,v}$, $W_{om,oda}$ and $W_{om,l}$ exit directly to the ambient environment and are governed by a linear nozzle equation with constant k_{om} and manifold and ambient pressure difference (6). The flow of liquid water leaving the manifold (7) is modeled to be dependent on the gas mass flow, the liquid water mass $m_{om,l}$ and a constant δ_l [7].

$$X_i = \frac{p_{v,i}}{p_i - p_{v,i}} \frac{R_{air}}{R_v} \tag{4}$$

$$p_v^{sat} = \exp\left(17.2799 - \frac{4102.99}{\vartheta + 237.431}\right) 0.611657\times 10^3 \tag{5}$$

$$W_{om} = k_{om}\left(p_{om} - p_{amb}\right) \tag{6}$$

$$W_{om,l} = \delta_l W_{om} m_{om,l} \tag{7}$$

Partial pressures of dry gas $p_{om,oda}$ and vapor $p_{om,v}$ are gained by a mass balance and the ideal gas law (8) with manifold volume V_{om} and the vapor gas constant R_v. ODA is approximated as air with gas constant R_{oda}=R_{air}. Condensation is considered happening instantaneously leading to the condensate mass $m_{om,l}$. The outlet manifold pressure is the sum of oda and vapor partial pressures $p_{om} = p_{om,oda} + p_{om,v}$.

$$\frac{dm_{om,oda}}{dt} = W_{ca,oda} - W_{om,oda}\,, \qquad W_{om,oda} = \frac{1}{1+X_{om}} W_{om}$$

$$\frac{dm_{om,H2O}}{dt} = W_{ca,v} + W_{ca,l} - W_{om,v} - W_{om,l}\,, \quad W_{om,v} = \frac{X_{om}}{1+X_{om}} W_{om}$$

$$p_{om,oda} = \frac{T_{om} R_{oda}}{V_{om}} m_{om,oda} \tag{8}$$

$$p_{om,v} = \min\left(p_v^{sat}(T_{om}), m_{om,H2O}\frac{R_v T_{om}}{V_{om}}\right) \tag{9}$$

$$m_{om,l} = \max\left(0, m_{om,H2O} - p_v^{sat}(T_{om})\frac{V_{om}}{R_v T_{om}}\right) \tag{10}$$

3) Fuel Cell Stack Electrical Model

The stack voltage $U_{stack} = n_{cells} U_{cell}$ is the sum of all n_{cells} cell voltages. The cell voltage is modeled as $U_{cell} = U_{rev} - \eta_{act} - \eta_{\Omega}$ (11) with the reversible cell voltage U_{rev}, activation loss η_{act} [13] and ohmic loss η_{Ω} [14]. The membrane thickness is given by d_m and the active surface area by A_{sfc}. Parameters $\zeta_1,\ldots\zeta_4$ and $b_1,\ldots b_3$ have been identified using experimental data.

$$\begin{aligned} U_{rev} &= 1.229 - 0.85\cdot 10^{-3}\left(T_{stack} - 298.15\right) + 4.3\cdot 10^{-5} T_{stack}\left(\ln\tfrac{p_{H2}}{p_0} + \tfrac{1}{2}\ln\tfrac{p_{O2}}{p_0}\right) \\ \eta_{act} &= \zeta_1 + \zeta_2 T_{stack} + \zeta_3 T_{stack}\ln\left(p_{O2} e^{(498/T_{stack})}/5.08\cdot 10^{-6}\right) + \zeta_4 T_{stack}\ln\left(I_{stack}\right) \\ \eta_{\Omega} &= \frac{d_m}{\left(b_1\lambda_m - b_2\right)} e^{-b_3\left(\frac{1}{303} - \frac{1}{T_{stack}}\right)} \frac{I_{stack}}{A_{sfc}} \end{aligned} \tag{11}$$

4) Fuel Cell Stack Thermal Model

An energy balance (12) leads to the fuel cell stack temperature T_{stack}. The stack has a heat capacity of C_{st}. The heat generated through the chemical reaction is given by the

chemical energy of hydrogen (HHV) and stack electrical energy. The stack is cooled by convective cooling with coolant mass flow $W_{cool} = W_{int}$ and specific heat capacity c_{cool}. The coolant stack inflow temperature is $T_{stackin}$. The coolant leaves the stack at stack temperature. Air, cathode water, vapor and oda gas are assumed to leave the stack at stack temperature as well. Air enters the stack at temperature T_{im}. Oda gas is approximated as air with specific heat capacity $c_{oda} = c_{air}$. The stack is very well insulated. So, heat transfer to surroundings is neglected. Enthalpy of evaporation is h_0.

$$\begin{aligned} C_{st}\frac{dT_{st}}{dt} &= \left(1.48\, n_{cells} - U_{stack}\right) I_{stack} \\ &+ W_{cool} c_{cool}\left(T_{stackin} - T_{stack}\right) \\ &+ W_{im} c_{air}\left(T_{im} - T_0\right) - W_{oda} c_{oda}\left(T_{stack} - T_0\right) \\ &- W_{ca,l} c_l \left(T_{stack} - T_0\right) - W_{ca,v}\left(h_0 + c_v\left(T_{stack} - T_0\right)\right) \end{aligned} \tag{12}$$

5) Fuel Cell Stack Anode and Cathode Model

Anode pressure $p_{an} = p_{H2} + p_{an,v}$ is the sum of hydrogen and vapor partial pressures and is governed by mass conservation (13) and the ideal gas law with R_{H2} being the hydrogen gas constant. In operation a mass flow $W_{H2rct} = (M_{H2} I_{stack} n_{cells})/(2F)$ of hydrogen is consumed. The stack is operated dead-ended and the system behavior is mimicked by a proportional controller for anode pressure p_{an} with hydrogen inlet mass flow W_{H2in}, anode reference pressure p_{an_ref} and controller gain k_{an} (14). Condensation is modeled happening instantaneously [5] if the vapor pressure exceeds saturation vapor pressure. The mass of condensate and the vapor partial pressure are modeled according to (9) and (10) with water mass (13). The anode water activity a_{an} is modeled as $a_{an} = p_{an,v}/p_v^{sat}$.

$$\frac{dm_{an,H2O}}{dt} = -W_{mem} \text{ and } \frac{dp_{H2}}{dt} = \frac{T_{stack} R_{H2}}{V_{an}}\left(W_{H2in} - W_{H2rct}\right) \tag{13}$$

$$W_{H2in} = k_{an}\left(p_{an\_ref} - p_{an}\right) \tag{14}$$

The cathode inlet mass flows of oxygen and nitrogen are governed by the mass fractions x_{O2} and x_{N2} assuming dry inlet air consisting of 21% of oxygen and 79% of nitrogen. The cathode exit mass flow W_{ca} is modeled as a 3-phase-flow (15) and is governed by a linear nozzle equation similar to (2) with constant k_{ca} and pressure difference $(p_{ca} - p_{om})$. Liquid water mass flow $W_{ca,l}$ is modeled according to (7). Cathode pressure $p_{ca} = p_{O2} + p_{N2} + p_{ca,v}$ is the sum of oxygen, nitrogen and vapor partial pressures and is governed by mass conservation (16) and the ideal gas law [5]. In operation a mass flow $W_{O2rct} = (M_{O2} I_{stack} n_{cells})/(4F)$ of oxygen is consumed and $W_{H2Orct} = (M_{H2O} I_{stack} n_{cells})/(2F)$ of water is generated. Condensation happens instantaneously. The vapor partial pressure and liquid mass in the cathode is modeled according to (9) and (10) using the water mass $m_{ca,H2O}$ in (16).

$$\begin{bmatrix} W_{im,O2} \\ W_{im,N2} \end{bmatrix} = \begin{bmatrix} x_{O2} \\ x_{N2} \end{bmatrix} W_{im} \text{ and } \begin{bmatrix} W_{ca,O2} \\ W_{ca,N2} \\ W_{ca,v} \end{bmatrix} = \frac{1}{1 + X_{CA}} \begin{bmatrix} \frac{m_{O2}}{m_{O2}+m_{N2}} \\ \frac{m_{N2}}{m_{O2}+m_{N2}} \\ X_{CA} \end{bmatrix} W_{ca} \tag{15}$$

$$\begin{aligned} \frac{dm_{ca,H2O}}{dt} &= W_{mem} + W_{H2Orct} - W_{ca,v} - W_{ca,l} \\ \frac{dm_{O2}}{dt} &= W_{im,O2} - W_{O2rct} - W_{ca,O2} \\ \frac{dm_{N2}}{dt} &= W_{im,N2} - W_{ca,N2} \end{aligned}, \quad \begin{aligned} p_{O2} &= m_{O2}\frac{T_{stack} R_{O2}}{V_{ca}} \\ p_{N2} &= m_{N2}\frac{T_{stack} R_{N2}}{V_{ca}} \end{aligned} \tag{16}$$

6) Fuel Cell Stack Membrane Model

Membrane material is Nafion®. The membrane water mass flow W_{mem} (17) is caused by gradient driven diffusion and electro-osmotic drag of water from anode to cathode [14]. Diffusion constant D_{diff} depends on the membrane hydration λ_{mem} and stack temperature (18). The membrane water activity a_{mem} is modeled as the average between cathode and anode water activity [14] (with j=*mem, ca, an*).

$$W_{mem} = A_{sfc} M_w n_{cells}\left(\lambda_{mem}\frac{2.5}{22}\frac{I_{stack}}{A_{sfc}F} - \frac{\rho_{dry}}{M_{dry}} D_{diff}\frac{\lambda_{ca} - \lambda_{an}}{d_m}\right) \tag{17}$$

$$D_{diff} = e^{2416(1/303 - 1/T_{st})}\left(2.563 - 0.33\lambda_{mem} + 0.0264\lambda_{mem}^2 - 0.000671\lambda_{mem}^3\right)\cdot 10^{-6}$$

$$\lambda_j = \begin{cases} 0.043 + 17.81 a_j - 39.85 a_j^2 + 36.0 a_j^3 & 0 < a \le 1 \\ 14 + 1.4\left(a_j - 1\right) & 1 < a \le 3 \end{cases} \tag{18}$$

7) Electrical Load Model

The stack is connected to a controllable ohmic load drawing a current as requested by a reference. An internal controller quickly adjusts the load resistance. To prevent numerical problems, the load is modeled as a first order transfer function with time constant T_L.

B. Cooling System Model

As shown in figure 1 the cooling system consists of an inner and an outer cooling loop that are interconnected by an counter-flow heat exchanger also called intercooler. In the inner loop pipes connect the intercooler and the stack.

1) Inner Cooling Loop Model

The cooling pump in the internal cooling circuit is controlled such that the cooling temperature difference across the stack equals the reference signal given by the stack manufacturer. The pump generates a coolant mass flow W_{int}, which is limited to a minimum of $W_{int,min}$ and a maximum of $W_{int,max}$. The cooling pump controller is modeled as a proportional and integral controller with anti-windup to prevent integrator windup. The pipes are modeled according to [13] and are considered perfectly insulated (20) with specific heat capacity c_{int} and $m_{pipe,i}$ being the mass of coolant in pipe i, the coolant inlet temperature $T_{pipein,i}$ and the pipe outlet temperature $T_{pipe,i}$. Using notation of figure 1 the temperature of pipe IL1 is $T_{stackin}$ and of pipe IL2 is $T_{stackout}$. The indices for the model equations (20) are i=IL1, IL2.

$$m_{pipe,i} c_{\text{int}} \frac{dT_{pipe,i}}{dt} = W_{\text{int}} c_{\text{int}}\left(T_{pipein,i} - T_{pipe,i}\right) \tag{20}$$

2) Outer Cooling Loop Model

The outer loop consists of an air-cooled heat exchanger (cooler) that cools the coolant to a temperature of T_{cooler} and pipes that connect the cooler with the intercooler. In a cooling valve warm coolant from the intercooler and cold cooling fluid from the cooler can be mixed. Warm coolant bypasses the cooler such that is does not cool down. As the bypass pipe is very short as compared to the other pipes its dynamics are neglected. The cooler is modeled as a pipe as well (21). The heat transferred to the surroundings is modeled by the coefficient k_{cooler} and the difference of cooler to ambient temperature T_{amb}. The mass flow in the external cooling loop is W_{ext} and the specific heat capacity of the coolant is c_{ext}. Using

notation of figure 1 the temperature of pipe OL1 is T_{ICin} and of pipe OL2 is T_{ICout}. The indices for the model equations (21) are i=OL1, OL2.

$$\begin{aligned} m_{pipe,i}c_{ext}\frac{dT_{pipe,i}}{dt} &= W_{ext}c_{ext}\left(T_{pipein,i}-T_{pipe,i}\right) \\ m_{cooler}c_{ext}\frac{dT_{cooler}}{dt} &= u_{valve}W_{ext}c_{ext}\left(T_{ICout}-T_{cooler}\right)-k_{cooler}\left(T_{cooler}-T_{amb}\right) \end{aligned} \tag{21}$$

In pipe OL2 the coolant for the hydrogen recirculation pump mixes with the coolant of the intercooler outflow. This temperature mixture is modeled by a stationary energy balance (22) with thermal input of the hydrogen pump and assuming that the mass flow through the recirculation pump W_{extH2} is 6% of W_{ext}. $T_{c,out}$ is the intercooler outlet temperature. The mass flow through the intercooler W_{extIC} is taken as 94% of the mass flow in the external cooling loop.

$$W_{ext}T_{ICout} = W_{extH2}\left(T_{ICin}+\frac{\dot{Q}_{H2\,pump}}{W_{extH2}c_{ext}}\right)+W_{extIC}T_{c,out} \tag{22}$$

3) Cooling Valve Model

The mixing temperature of the cooling valve is modeled by a stationary energy equation (23) as the mixing process is considered very fast. The valve splits the mass flow through cooler and bypass given by its actual position u_{valve}.

$$W_{ext}T_{pipein,OL1} = u_{valve}W_{ext}T_{cooler}+\left(1-u_{valve}\right)W_{ext}T_{ICout} \tag{23}$$

The cooling valve has limited dynamics. This results in a limited speed of opening and closing the valve. For small changes in position it behaves linearly. It is modeled having a constant opening and closing speed du_{max} for large changes and behaves like a first order transfer function for small changes in valve position (24). Reference position is $u_{valve,ref}$.

$$\frac{du_{valve}}{dt} = \int \begin{cases} du_{\max} & k_{valve}\left(u_{valve,ref}-u_{valve}\right) > du_{\max} \\ k_{valve}\left(u_{valve,ref}-u_{valve}\right) & otherwise \\ -du_{\max} & k_{valve}\left(u_{valve,ref}-u_{valve}\right) < -du_{\max} \end{cases} \tag{24}$$

4) Intercooler Model

The counter-flow heat exchanger that connects the inner and outer cooling loop is considered static. This assumption is motivated by the high mass flows in the cooling system and the small coolant mass inside the intercooler as compared to the entire cooling system. For modeling counter-flow heat exchangers the effectiveness NTU method [10] has shown very good results. NTU is the number of transfer units, which is an important parameter in heat exchanger design and modeling. The effectiveness NTU is advantageous as outlet temperatures are calculated explicitly on inlet temperatures and cooling mass flows. Heat flow is gained by the inlet temperature differences, the minimum heat capacity flow and the effectiveness ε. The outlet temperatures (25) are gained by the heat capacity flow of the hot side $C_h=W_{int}c_{int}$ and the cold side $C_c=W_{extIC}c_{ext}$. The outlet temperatures are $T_{c,out}$ and $T_{h,out}$ for cold and hot side. The inlet temperatures are $T_{c,in}=T_{ICin}$ and $T_{h,in}=T_{stackout}$.

$$\begin{aligned} T_{c,out} &= T_{c,in}+\frac{\varepsilon C_{\min}}{C_c}\left(T_{h,in}-T_{c,in}\right) \\ T_{h,out} &= T_{h,in}-\frac{\varepsilon C_{\min}}{C_h}\left(T_{h,in}-T_{c,in}\right) \end{aligned} \tag{25}$$

$$C_{\min}=\min\left(C_h,C_c\right),\ C_{\max}=\max\left(C_h,C_c\right),\ C^*=\frac{C_{\min}}{C_{\max}},\ NTU=\frac{UA}{C_{\min}}$$

The heat exchanger effectiveness ε is obtained by (26). UA is the parameter describing the heat transfer.

$$\varepsilon = \begin{cases} \dfrac{NTU}{1+NTU} & C^*=1 \\ \dfrac{1-\exp\left(-NTU\left(1-C^*\right)\right)}{1-C^*\exp\left(-NTU\left(1-C^*\right)\right)} & otherwise \end{cases} \tag{26}$$

III. Model Identification

As shown in the previous paragraphs, the fuel cell system model as well as the cooling system model has parameters describing the plant geometry such as manifold volumes and coolant masses and parameters for mass flows, polarization curve and the intercooler. Parameters $\zeta_1,\ldots\zeta_4$ and $b_1,\ldots b_3$ for the polarization curve, k_{im}, k_{ca}, k_{om} and k_{an} for the mass flows have been identified by a least square error minimization such that simulated inlet and outlet manifold as well as cathode and anode pressure and simulated stack voltage fit to experimental data. Cathode pressure cannot be measured, therefore, it is assumed as the arithmetic mean of the inlet and outlet manifold pressures. The objective function (27) has scaling factors for pressure μ_p and voltage μ_U such that quadratic errors of the same order are gained.

$$\begin{aligned} J_{FCS,i} &= \mu_p\left(p_{im,\exp,i}-p_{im,sim,i}\right)^2+\mu_p\left(p_{ca,\exp,i}-p_{ca,sim,i}\right)^2 \\ &\quad+\mu_p\left(p_{om,\exp,i}-p_{om,sim,i}\right)^2+\mu_p\left(p_{an,\exp,i}-p_{an,sim,i}\right)^2 \\ &\quad+\mu_U\left(U_{stack,\exp,i}-U_{stack,sim,i}\right)^2 \\ J_{FCS} &= \sum_i J_{FCS,i} \end{aligned} \tag{27}$$

Simulation results of the stationary fuel cell system model after identification of the polarization curve for different sets of stoichiometry and stack inlet cooling temperature are shown in figure 2. The results for inlet as well as outlet manifold and anode pressure are shown in figure 3. As the comparison between experimental data and simulation model shows, the model fits the experimental data very well.

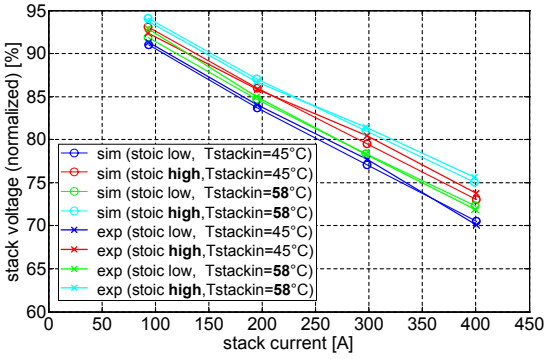

Figure 2. Comparison of experimental and simulation model fuel cell stack polarization curves for different sets of stack inlet temperature (45 and 58°C) and cathode stoichiometry (high and low stoic)

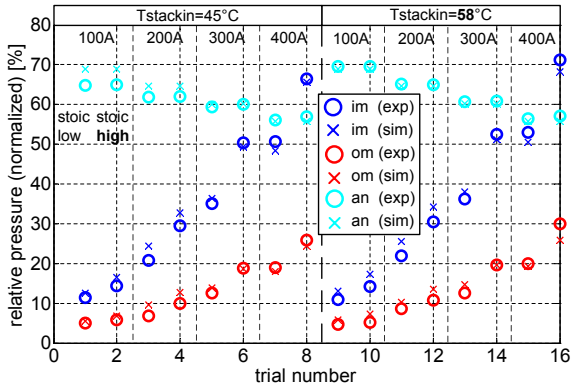

Figure 3. Comparison of experimental and simulation inlet manifold (im), outlet manifold (om) and anode (an) pressures; 16 sets of combinations of stack current, stack inlet temperature and cathode stoichiometry (stoic)

To capture the slow temperature dynamics in the simulation model as well, the stack heat capacity was determined by comparing stack temperature of simulation and experiment until results agreed well. For determining the stack heat capacity cooling mass flow and inlet temperature as well as stack current were prescribed. Simulation results with a PI-controlled cooling pump and stack current, stoichiometry and the coolant inlet temperature prescribed are shown in figure 4 and 5. The dynamic simulation results show that deviations between model and experiment in terms of pressure as well as stack voltage are small. The dynamic simulation model fits the experimental data very well.

1) Identification of the Intercooler Model

Parameter *UA* of the intercooler model has been identified by a least square error minimization as well. For model identification it was assumed that temperature measurement errors compensate as the temperature difference across the heat exchanger is taken. The cooling mass flow $W_{int,measure}$ of the internal cooling loop can be considered an exact measurement. The cooling mass flow in the external cooling loop $W_{ext,measure}$, however, is corrected by a constant factor α to minimize the difference between the stationary energy balances of hot and cold side (28). The stationary balance is determined by cooling mass flow, specific heat capacity of the coolant and the temperature difference.

$$J_Q = \sum_i \dot{Q}_{h,i} - \dot{Q}_{c,i} = \sum_i W_{\text{int},measure,i} c_{\text{int}} \Delta T_{\text{int},measure,i} - \alpha W_{ext,measure,i} c_{ext} \Delta T_{ext,measure,i} \quad (28)$$

Heat flows resulting from an energy balance about inner and outer cooling loop are shown in figure 6. Using $W_{int,measure}$, the corrected mass flow $\alpha W_{ext,measure}$ and temperatures of hot and cold fluid at in- and outlet the intercooler parameter *UA* has been identified by a least square error minimization with objective function (29). Coolant mass flows and temperatures at the heat exchanger inflow at inner and outer loop were prescribed. *UA* has been fit to minimize the difference between simulated and measured coolant temperatures at the intercooler outflows.

$$J_T = \sum_i \left(T_{hout,\exp,i} - T_{hout,sim,i}\right)^2 + \left(T_{cout,\exp,i} - T_{cout,sim,i}\right)^2 \quad (29)$$

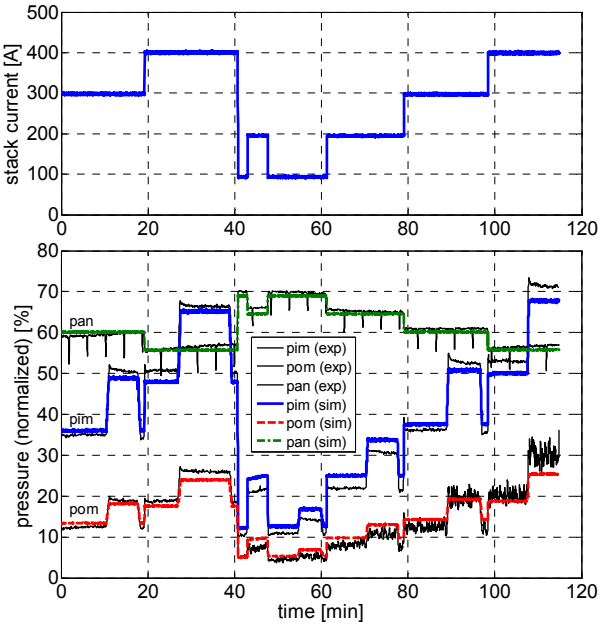

Figure 4. Simulation results dynamic fuel cell system model: experimental stack current profile also used as current profile for the simulation model (top); in- and outlet manifold and anode pressure of simulation and experiment (bottom)

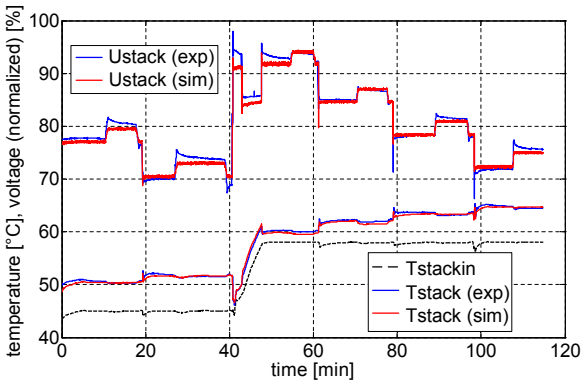

Figure 5. Simulation results fuel cell system model: stack cooling and stack temperature and stack voltage of simulation and experiment

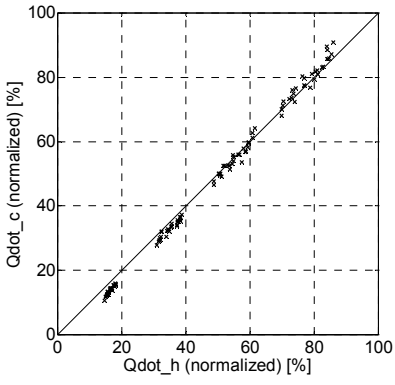

Figure 6. Stationary heat flows leaving the inner cooling loop (Qdot_h) and being brought into the outer cooling loop (Qdot_c) at the intercooler with corrected cooling mass flow of the outer cooling loop

A comparison of simulation results and experimental data for different sets of stack current, outer loop cooling temperature and cooling mass flow are shown in figure 5. An increase of stack current leads to an increase of coolant temperature in the inner loop as the thermal load is increased which can be seen by the polarization curve in figure 2.

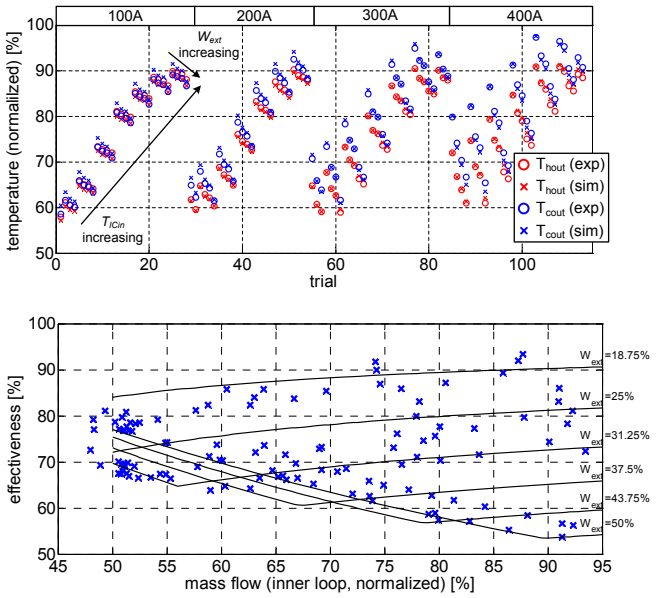

Figure 7. Comparison of experimental and simulation model outlet temperature of inner (T_{hout}) and outer (T_{cout}) cooling loop; for different sets of stack current, outer loop cooling temperature T_{ICin} and outer loop cooling mass flow W_{ext}; cathode stoichiometry was kept constant (top); effectiveness of the intercooler model for all experimental trials and shown for various cooling mass flows in the inner and outer loop (bottom)

As shown in figure 7 the intercooler simulation results of the stationary model fit the experimental data very well. Furthermore, the heat exchanger effectiveness changes significantly within an interval of 50-95%. Figure 7 also shows the evolution of the effectiveness for constant mass flows W_{ext} in the outer loop while the flow in the inner loop W_{int} is varied. For constant W_{ext} the effectiveness could be approximated by a constant, however still can change significantly depending on the choice of W_{ext}. As future controller designs possibly work with various pump speeds, a simulation model that is correct over the whole operating range of the fuel cell system is necessary. Therefore, the effectiveness is modeled as in [10] being dependent on cooling mass flows. For the dynamic simulation model parameters such as manifold, cathode and anode volumes and pipe coolant masses were determined by the system geometry and data provided by the manufacturer.

IV. Cooling Controller Architecture

For the design of a stack inlet cooling temperature control the fuel cell system is considered a stack current dependent heat source generating a heat flow into the inner cooling loop as shown in figure 1. Evaluating the cooling system model at steady state and neglecting the hydrogen compressor's influence, the steady state valve position u_{ss} to reach a certain stack inlet temperature $T_{stackin,ref}$ can be obtained by (30) with the cooler temperate T_{cooler}.

$$u_{ss} = \frac{\dot{Q}_{FC}}{C_c\left(\frac{\dot{Q}_{FC}}{C_h} - \frac{\dot{Q}_{FC}}{\varepsilon C_{\min}} + \frac{\dot{Q}_{FC}}{C_c} + T_{stackin,ref} - T_{cooler}\right)} \tag{30}$$

An estimation of the thermal load is obtained by (31) with the actual electrical power $P_{stack} = U_{stack} I_{stack}$ and a cell voltage corresponding to the lower heating value (LHV) of hydrogen as the stack is partly cooled by evaporation of product water in the cathode. The cooler temperature T_{cooler} is being measured. The heat exchanger effectiveness ε and heat capacity flows C_h, C_c and C_{min} are obtained by (25)-(26) using the measured cooling mass flows W_{int} and W_{extIC}.

$$\dot{Q}_{FC} = U_{LHV}\, n_{cells} I_{stack} - P_{stack} \tag{31}$$

The control law proposed is a combination of the nonlinear feedforward control and a linear proportional and integral controller with an anti-windup to prevent integrator windup (32). The anti-windup circuit is active for controller outputs greater than 100% (a_{windup}=100%-u) and outputs less than 0% (a_{windup} = 0%-u) and is inactive otherwise (a_{windup}=0). The controller gains $k_p > 0$ and $k_i > 0$ add with a negative sign as shown in (32) as the cooling valve needs to open for negative control errors ($T_{stackin} > T_{stackin,ref}$) and to close for positive ones.

$$u = u_{ss} - k_p\left(T^{ref}_{stackin} - T_{stackin}\right) - k_i \int T_{stackin,ref} - T_{stackin} - a_{windup}\, dt \tag{32}$$

A constant cooling mass flow W_{ext} in the outer loop is set for the controller. Increasing the cooling mass flow would improve the cooling system dynamics as states in (21). Higher mass flows reduce the time constants for temperature in the pipe volumes. Higher pump speeds, however, result in higher power consumption. Nevertheless, the stack temperature can be set by either actuating the cooling valve or actuating the pump within certain limits set by the intercooler. This circumstance can be exploited for future control designs such that an optimal balance between pump and valve is found to optimize for power consumption or time. Here, the cooling mass flow W_{ext} is set constant.

V. Simulation Results

The simulation model is developed and run in Matlab/Simulink®. The controller for stack inlet cooling temperature is connected with the nonlinear fuel cell system model. The simulation was run for a stack cooling reference temperature of 55°C and high cathode stoichiometry. Figure 8 shows the simulation results of three controller variants:

(A) PI-control activated, feedforward control deactivated
(B) PI-control deactivated and feedforward control activated
(C) PI- and feedforward control activated.

For a constant stack cooling reference temperature of 55°C a stack current profile as shown in figure 8 was taken to test the controller for different thermal loads. With a pure feedforward control (type B) stack temperature in steady state is close to the reference temperature. The control behavior is further improved by a linear PI-controller (type C). The temperature matches the reference in steady state and under- as well as overshoots are less than in the case of a linear controller without feedforward control (type A).

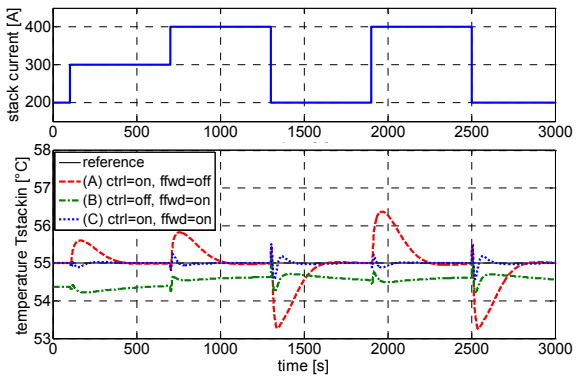

Figure 8. Simulation results of stack cooling controller for 3 controller configurations; stack current profile (top), stack cooling temperature (bottom)

VI. CONCLUSION

A polymer electrolyte membrane fuel cell system electrically connected to an ohmic electronic load is connected to a coupled double-loop-cooling system with two different coolants of different specific heat capacity. The cooling loops are interconnected by a counter-flow heat exchanger (intercooler). The entire system model is derived based on physical principals and has been modeled in Matlab/Simulink®. The fuel cell system model has been fit to experimental data with very good agreement. The intercooler is modeled by the effectiveness NTU method by which a static nonlinear model is obtained. This model is valid over the entire operating range of the fuel cell system. Outlet temperatures are calculated explicitly based on input variables such as temperatures and mass flows. The intercooler model has been fit to experimental data and shows very good agreement over the entire operating range. A linear PI-controller with nonlinear feedforward control is proposed to control for stack inlet cooling temperature. The temperature controller is implemented in the nonlinear simulation model. The fuel cell and cooling system model will by used for future controller designs such as for an optimal change of stack temperature operating points or for an optimal system heat up.

REFERENCES

[1] E. Vredenborg, H. Lüdders and F. Thielecke, "Methodology for Sizing and Simulation of complex Fuel Cell Systems" orig.(german) "Methodik zur Auslegung und Simulation komplexer Brennstoffzellensysteme", Deutscher Luft- und Raumfahrtkongress 2010, DocumentID: 161248.

[2] J. Bleil, "Fuel Cells for onboard Power Supply of Aircraft", orig. (german) "Brennstoffzellen zur Bordstromversorgung von Flugzeugen", HZwei-Das Magazin für Wasserstoff und Brennstoffzellen, 04/2007

[3] R. Borup et al., "Scientific Aspects of Polymer Electrolyte Fuel Cell Durability and Degradation", Chem. Rev, vol. 107, pp. 3904-3951, 2007

[4] A. J. del Real, A. Arce, and C. Bordons, "Development and experimental validation of a PEM fuel cell dynamic model", Journal of Power Sources, vol. 173, pp. 310-324, 2007

[5] J. T. Pukrushpan, A. G. Stefanopoulou and H. Peng, Control of Fuel Cell Power Systems. London: Springer-Verlag, 2004.

[6] A. Y. Karnik, J. Sun, A. G. Stefanopoulou and J. H. Buckland, "Humidity and Pressure Regulation in a PEM Fuel Cell Using a Gain-Scheduled Static Feedback Controller", IEEE Transactions on Control Systems Technology, vol. 17, No. 2, pp. 283-297, 2009

[7] M. Schultze and J. Horn, "A Control Oriented Simulation Model of an Evaporation Cooled Polymer Electrolyte Membrane Fuel Cell System", 18th IFAC World Congress, Milan, Italy, 2011

[8] M. Schultze and J. Horn, "Current Control of a PEMFC System connected to an Electrical Load through a DC/DC Converter", 19th Mediterranean Conference on Control & Automation, pp. 55-60, 2011

[9] J. Niemeyer, Model Predicitve Control of a PEM-Fuel Cell System, orig. (german) Modellprädiktive Regelung eines PEM-Brennstoffzellensystems, Schriften des Instituts für Regelungs- und Steuerungssysteme, Universität Karlsruhe, Band 05, 2009

[10] R. K. Shah and D. P. Sekulic, Fundamentals of Heat Exchanger Design, Hoboken, NJ: John Wiley & Sons, 2003

[11] J. Nolan and J. Kolodziej, "Modeling of an automotive fuel cell thermal system", Journal of Power Sources, vol. 195, pp. 4743-4752, 2010

[12] H. D. Baehr and S. Kabelac, Thermodynamics, orig. (german) Thermodynamik, Berlin: Springer-Verlag, 2006

[13] J. C. Amphlett, R. M. Baumert, R. F. Mann, B. A. Peppley and P. R. Roberge, "Performance Modeling of the Ballard Mark IV Solid Polymer Electrolyte Fuel Cell", J. Electrochem. Soc., vol. 142, pp. 1-8, 1995

[14] R. O'Hayre, S.-W. Cha, W. Colella and F. B. Prinz, Fuel Cell Fundamentals. Hoboken, NJ: John Wiley & Sons, 2009.

TABLE I. FUEL CELL SYSTEM MODEL PARAMETERS

Parameter	DESCRIPTION	Value
M_{H2O}	molar mass of water	18.0153 g/mol
M_{O2}	molar mass of oxygen	31.9988 g/mol
M_{N2}	molar mass of nitrogen	28.0134 g/mol
M_{H2}	molar mass of hydrogen	2.01588 g/mol
R_v	gas constant of vapor	461.5 J/kg/K
R_{O2}	gas constant of oxygen	259.8 J/kg/K
R_{N2}	gas constant of nitrogen	296.8 J/kg/K
R_{H2}	gas constant of hydrogen	4124.49 J/kg/K
R_{air}, R_{oda}	gas constant of air, ODA	287.058 J/kg/K
F	Faraday's constant	96485.3 C/mol
c_{air}, c_{oda}	specific heat capacity of air, ODA	1004.7 J/kg/K
c_l	specific heat capacity of water	4181.9 J/kg/K
c_v	specific heat capacity of vapor	1864.6 J/kg/K
h_o	enthalpy of evaporation	2500.9×10^3 J/kg
n_{cells}, A_{sfc}	number of cells in the stack, active surface area	
d_m	membrane thickness	
V_{im}, V_{om}, V_{ca}, V_{an}	volume of inlet and outlet manifold, stack cathode and anode	
C_{st}	fuel cell stack heat capacity	
c_{int}, c_{ext}	coolant specific heat capacity in the inner and outer cooling loop	
W_i	mass flow leaving cathode and anode (i=*ca, an*), in- and outlet manifold (i=*im,om*), mass flow controller (i=*MFC*)	
$W_{i,oda}$, $W_{i,l}$, $W_{i,v}$	mass flow of ODA, liquid water and vapor in cathode and outlet manifold (i=*ca, om*)	
W_{int}, W_{ext}	coolant mass flow inner and outer cooling loop	
$m_{pipe,i}$, m_{cooler}	mass of coolant in pipe i (i=*IL1, IL2, OL1, OL2*), mass of coolant in the cooler	
p_i	pressure in volume i (i=*im, ca, an, om*)	
$m_{i,H2O}$	mass of total water in volume i (i=*ca, an, om*)	
$m_{i,l}$	condensate mass in i (i=*ca, an, om*)	
m_{O2}, m_{N2}	mass of oxygen, nitrogen in cathode	
$m_{pipe,i}$,m_{cooler}	coolant mass in i (i=*IL1, IL2, OL1, OL2*) and cooler	
p_{O2}, p_{N2}, p_{H2}, $p_{i,v}$	partial pressure of oxygen, nitrogen, hydrogen and vapor in cathode, anode and outlet manifold (i=*ca, an, om*)	
p_{amb}, T_{amb}	ambient pressure and temperature	
T_i	temperature in volume i (i=*im, stack, om*)	
$T_{pipe,i}$, T_{cooler}	temperature in pipe i (i=*IL1, IL2, OL1, OL2*) and cooler	
T_{MFC}, T_L	time constant of mass flow controller, electrical load	
k_{cooler}	heat transfer coefficient of the cooler	
k_{im}, k_{om}, k_{ca}, k_{an}	mass flow coefficients for inlet- and outlet manifold, cathode and anode	
$\zeta_1,\ldots\zeta_4$	coefficients for stack voltage activation loss	
$b_1,\ldots b_3$	coefficients for stack voltage ohmic loss	